

NUMERICAL INVESTIGATION ON TWO-PHASE FLUID FLOW CHARACTERISTICS OF EVAPORATOR DISTRIBUTOR WITH R404A AND R744 REFRIGERANTS

M. H. SOKUCU^(a), M. C. ÜNAL^(b), A. B. OLCAY^(b), H. ONBAŞIOĞLU^{(a)*}

^(a)Friterm Inc. Research and Development Department, Istanbul, 34957, TURKEY

^(b)Yeditepe University, Department of Mechanical Engineering, Istanbul, 34755, TURKEY

*Corresponding Author: Dr. Hüseyin Onbaşıoğlu, huseyinonbasioglu@friterm.com

ABSTRACT

Evaporators play a key role in refrigeration units and they are typically determined in accordance with the size of cooling systems. While evaporators can have multiple circuits for refrigerant to flow through, each circuit is designed to have equal amount of liquid refrigerant so that desired heat can be absorbed from the surrounding efficiently and ensuring that all the refrigerant is completely evaporated into gaseous phase. However, when evaporator's circuits receive non-uniform refrigerant from a distributor placed between the expansion valve and the evaporator, this non-uniform flow can yield reduction in capacity and COP of refrigeration system. In the present study, an evaporator distributor will be numerically studied by using two different refrigerants, R744 and R404A, for the purpose of identifying the difference in behavior of these refrigerants. The quality of mixture for refrigerants will be varied by taking corresponding qualities for evaporation temperatures -8°C , -18°C and -25°C to identify the relation between refrigerant's quality and mass distribution of refrigerant in each tube of the distributor. In addition to use of two different refrigerants, nozzle position of the distributor was changed from 0.01 mm to 2.01 mm and 4.01 mm to evaluate the effect of nozzle placement on mass flow rate uniformity at the distributor exits for an evaporation of -8°C . It was realized that the effect of evaporation temperature was only significant for R404A study since -8°C evaporation temperature provided most uniform mass uniformity at the distributor exit. It was also noticed that nozzle positions of 0.01, 2.01 and 4.01 mm were only significant for R404A fluid flow simulations since both 2.01 and 4.01 mm nozzle locations resulted in nearly 40% deviation in mass flow rate at distributor exits.

Key words: Evaporator distributor, CFD, two phase flow, R744, refrigeration

1. INTRODUCTION

Evaporators are integral part of refrigeration systems since cooling can be provided thru these machines and they generally possess multiple circuits to supply designed cooling capacity to the desired environment. While these circuits are essential part of an evaporator, use of evaporator distributor becomes crucial to distribute the incoming refrigerant to the circuits of an evaporator uniformly. Therefore, an evaporator distributor is a machine part with one inlet and multiple exits and it is placed between expansion valve and evaporator to distribute refrigerant to the evaporator circuits. Refrigerant enters to the evaporator distributor as a mixture of liquid and vapor phases and passes through a nozzle section before splitting into several exit tubes. The orientation of the distributor and density differences between liquid and vapor phases of refrigerant directly affect mass flow rate uniformity at distributor exit. In literature, the study was performed to compare single phase and two-phase flow streams in terms of mass flow rate uniformity (Poggi, Macchi-Tejeda, Maréchal, Leducq, & Bontemps, 2007). It was reported that a single phase flow was distributed homogeneously while two phase flow was non-uniform based on quality of inlet stream. In another study, mixture of air and water were used in a two-dimensional geometry to investigate void fraction ratios in two circuits (Gang Li, Frankel, Braun, & Groll, 2002). When two-phase flow needs to be divided into multiple portions, each fluid stream can have different mass flow rate due to geometric factors of a distributor, quality of fluid stream and presence of gravity (Aziz, Miyara, & Sugino, 2012). Both different quality of refrigerant and variety of flow rates at the evaporator distributor inlet were also evaluated to understand the implications of mass flow rate non-uniformity on evaporator capacity (Nakayama, Sumida, Hirakuni, & Mochizuki, 2000). Gravitational and inertial effects of two-phase flow in evaporator distributor were examined (Fei & Hrnjak, 2004; Tompkins, Yoo, Hrnjak, Newell, & Cho, 2002). Besides, the capacity of evaporator was also measured when circuits of evaporators received non-uniform refrigerant (G. Li, Braun, Groll, Frankel, & Wang, 2002). It was documented that non-uniformity in mass flow rate caused air side flow characteristics

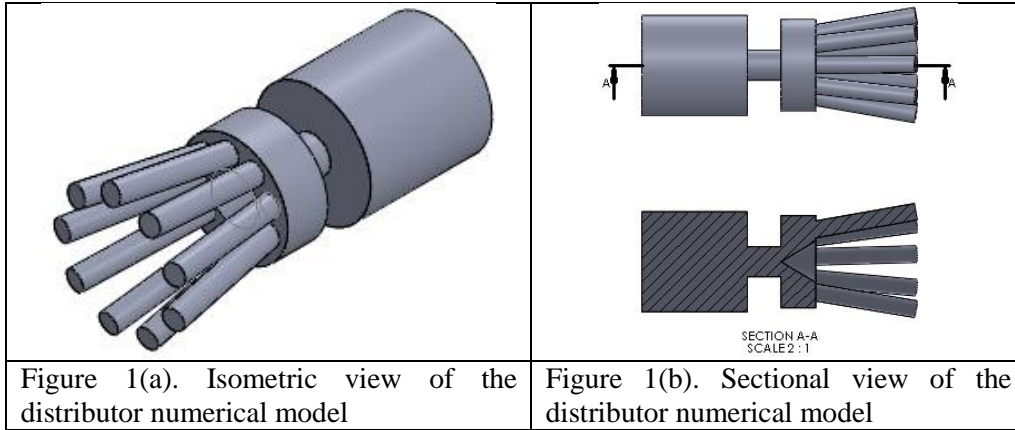
and 6% decrease in heat transfer rate implying the importance of uniform mass flow rate in each circuit of evaporator. Similarly, non-uniform mass flow rate distribution in evaporator circuits was studied and 10-15% decrease in coefficient of performance (COP) was determined (Kim, Braun, & Groll, 2009). The maldistribution in mass flow rate negatively affects heat transfer rate and pressure drop (Balasubramaniam, Ramé, Kizito, & Kassemi, 2006).

In the present study, motivated by the importance of uniform mass flow distribution in an evaporator distributor, a three dimensional computational fluid dynamics model was designed and generated. Two different working fluids, namely R404A and R744, were selected to identify the effect of working fluid on mass flow rate uniformity at several evaporation temperatures which in turn results in variation of quality of the fluid entering the distributor. Besides, a nozzle of a distributor was moved to several positions to determine how nozzle position affected mass flow rate distribution in exit tubes of the evaporator distributor for both R404A and R744.

2. MATERIALS AND METHODS

2.1. Geometry of an evaporator distributor

An evaporator distributor used in a commercial refrigeration system was selected to be studied to evaluate the mass flow rate distribution at the exit tubes of the distributor. Figure 1(a) shows isometric view of the evaporator distributor and sectional view of the distributor is given in Figure 1(b). As it can be seen, there is one inlet and 9 exits in the distributor.



2.2. Numerical model

A three-dimensional computational fluid dynamics model (CFD) was generated based on the solid model shown in Figure 1. Three different distributor geometries were obtained by changing the distance between apex of distributor conical member and nozzle outlet to evaluate the effect of distance on mass flow rate distribution at the distributor exit tubes. Specifically, distances were set to be 0.01 mm, 2.01 mm and 4.01 mm. Two common working fluids, namely *R404A* and *CO₂*, were utilized in the models as refrigerants. The CFD model was prepared for two-phase flow computations with ANSYS CFX© and segregated flow model was employed for the computational domain since liquid - vapor mixture would be separated from each other before entering into the distributor due to the density differences. Mass flow rates of fluid streams were defined as bulk mass flow rate to inlet areas and static pressure was entered to be 0 Pa at the outlet. Gravitational acceleration was activated and it was taken to be 9.81 m/s² in the +z direction. Reynolds number for the fluid flow in the distributor was much larger than the critical Reynolds number; therefore, flow was completely turbulent and k-ε turbulence model was employed for the two phase flow simulations (Equation & Models, 1993; Wilcox, 1993). This model is preferred because of its quickness and robustness compared to k-ω turbulence model. k- ε model equations are;

$$\frac{\partial}{\partial t} (\rho_m k) + \nabla * (\rho_m \vec{v}_m k) = \nabla * \left(\frac{\mu_{t,m}}{\sigma_k} \nabla k \right) + G_{k,m} - \rho_m * \varepsilon \quad (1)$$

$$\frac{\partial}{\partial t} (\rho_m \varepsilon) + \nabla * (\rho_m \vec{v}_m \varepsilon) = \nabla * \left(\frac{\mu_{t,m}}{\sigma_\varepsilon} \nabla \varepsilon \right) + \frac{\varepsilon}{k} (C_{1\varepsilon} G_{k,m} - C_{2\varepsilon} \rho_m) \quad (2)$$

Where the ρ_m is the mixture density and \vec{v}_m is the velocity that are calculated from,

$$\vec{v}_m = \frac{\sum_{i=1}^N \alpha_i \rho_i \vec{v}_i}{\sum_{i=1}^N \alpha_i \rho_i} \quad (3)$$

Where, $\rho_m = \sum_{i=1}^N \alpha_i \rho_i$, $\mu_{t,m} = \rho_m C_\mu \frac{k^2}{\varepsilon}$ and $G_{k,m} = \mu_{t,m} (\nabla \vec{v}_m + (\nabla \vec{v}_m)^T) / \nabla \vec{v}_m$. The constants are determined to be $C_\mu = 0.09$; $\sigma_\varepsilon = 1.30$; $\sigma_k = 1.00$; $C_{1\varepsilon} = 1.44$; $C_{2\varepsilon} = 1.92$. Details of the void fraction (i.e., ratio of gas flow area over total flow area) calculations using Zivi and Fauske correlations, two-phase flow and separated model equations were provided by (Sökücü, 2016). Three different evaporation temperatures of -8°C , -18°C and -25°C were chosen to study for R404A while 40°C was set for condensation temperature. Similarly, evaporation temperatures were selected to be -8°C , -18°C and -25°C for CO₂ while condensation temperatures were -8°C , -8°C and 10°C , respectively assuming a subcritical cycle. The simulations were performed for the same thermodynamic properties at -8°C evaporation temperature as shown in Table 1 and presuming that the coolers are performing the same thermal cooling capacity for the sake of comparing at similar practical conditions.

Table 1. Thermodynamic properties at -8°C evaporation temperature for R404A and CO₂

	R404A	CO ₂
T _{evap} [°C]	-8	-8
T _{cond} [°C]	40	10
T _{superheat} [°C]	5.2	5.2
T _{subcooling} [°C]	10	1
P _{evap} [kPa]	464.2	2800
x	0.328	0.164
inlet diameter	19 mm	19 mm
A _{distinlet} (m ²)	0.000283529	0.000283529
m [kg/s]	0.0424	0.023718
m _{gas} (kg/s)	0.0139072	0.003889752
m _{liquid} (kg/s)	0.0284928	0.019828248
ρ _{gas} (kg/m ³)	23.47	75.75
ρ _{liquid} (kg/m ³)	1180	972.6
Dynamic viscosity [Pa·s] lq	1.97E-04	1.20E-04
Dynamic viscosity [Pa·s] gas	1.11E-05	1.40E-05
Kinematic viscosity [m ² /s] lq	8.37E-06	1.58E-06
Kinematic viscosity [m ² /s] gas	4.72E-07	1.85E-07
Thermal conductivity [W/(m·K)]	8.26E-02	1.42E-01
Surface tension, σ _{gas-liquid} (N/m)	0.00455	0.01145
Molar mass (kg/kmol)	97.6	44
V Gas volumetric flow (m ³ /s)	0.000592552	5.13499E-05
(V)Liquid volumetric flow (m ³ /s)	2.41464E-05	2.03868E-05
(V)Total volumetric flow (m ³ /s)	0.000616699	7.17367E-05
G (total mass flux) (kgm ² /s)	149.5439244	83.652896183
β _{Volumetric Dryness}	0.960845639	0.715810107
α _(void fraction,armand)	0.800384418	0.596269820
α _(void fraction,zivi)	0.869262434	0.518223787
α _(void fraction,fauske)	0.775829981	0.412777531
α _(void fraction,mean)	0.815158944	0.509090379
V _{gassuperficialvelocity} (m/s)	2.089919352	0.181109901
V _{liquidsuperficialvelocity} (m/s)	0.085163998	0.071903991
V _{gasmeanvelocity} (m/s)	2.563818219	0.355751961
V _{liquidmeanvelocity} (m/s)	0.460741783	0.146470934
A _{distinletlq} (m ²)	5.24078E-05	0.000139187
A _{distinletgas} (m ²)	0.000231121	0.000144342

2.3. Studied parameters in the present work

Once a three-dimensional CFD model was produced, two different working fluids, three different evaporation temperatures and geometries were implemented to the model to evaluate the effects of working fluid and geometry differences on mass flow rate distribution at the exit tubes of an evaporator distributor. Specifically, R404A and CO₂ refrigerants were defined for fluid domain of the CFD model. Three different evaporation temperatures with different mixture qualities were identified at the nozzle exit to determine how liquid and vapor mixture splits into the exit tubes. Lastly, distance between apex of distributor conical member and nozzle outlet was defined to be 0.01, 2.01 and 4.01 mm. However, when distance between apex of distributor conical member and nozzle outlet was varied from 0.01 to 2.01 and 4.01mm, more elements were needed to be placed into the computational domain to fill the additional volume. Briefly, 300,000 to 400,000 tetrahedral and hexahedral elements were used in mesh placement of CFD models. In the present study two different mesh structures were also employed on computational domain as shown in Figure 2.

2.4. Identification of evaporator distributor exits

The outlets of the distributor exits were numbered as shown in Figure 2(c) so that mass flow rate values at the outlets can be calculated and compared with each other. Therefore, the effect of evaporation temperatures, nozzle positions and working fluids on mass flow distribution at the exit of an evaporator distributor is investigated in the present study.

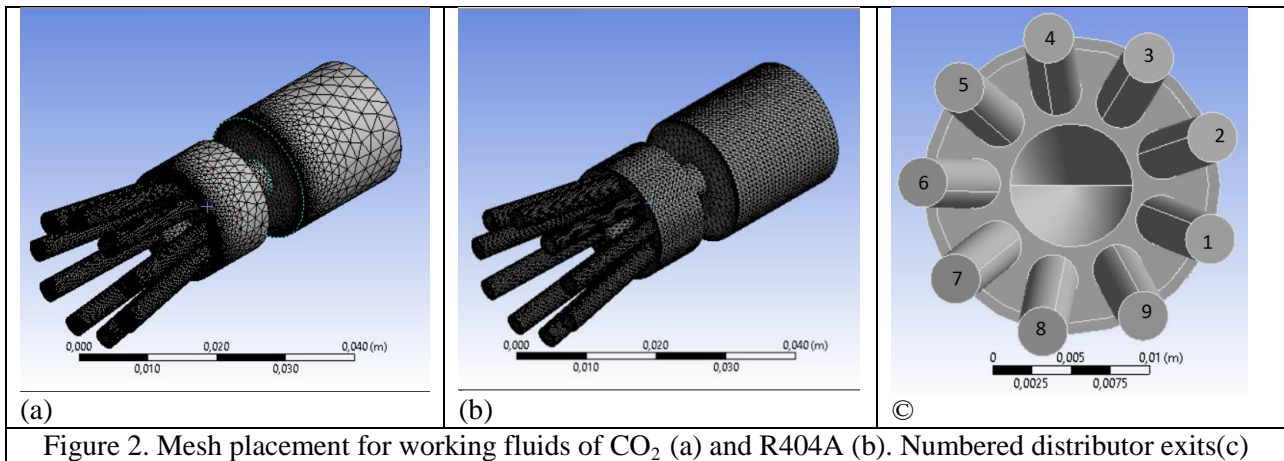


Figure 2. Mesh placement for working fluids of CO₂ (a) and R404A (b). Numbered distributor exits(c)

3. RESULTS AND DISCUSSION

In this part of the study, the numerical results are presented for two working fluids, three different evaporation temperatures and nozzle positions. Briefly, mass flow distribution characteristics of R404A and CO₂ are discussed based on the evaporation temperature and nozzle geometry positions.

3.1. The effect of evaporation temperature on mass flow rate distribution for R404A

Evaporation temperatures of -8°C, -18°C and -25°C for R404A were simulated for three different inlet mass flow rates, namely 0.0047, 0.0050, 0.0051 kg/s, respectively. Figure 4 shows void fractions for the same evaporation temperatures. Void fraction is being representation of vapor area to total area can influence mass flow rate distribution at the distributor exits. Void fraction in Figure 4 exhibits a decline for exit numbers 7, 8 and 9 indicating more area occupation by the liquid phase. Actually, these exit numbers were directly downward of the nozzle outlet and they were automatically exposed to the liquid phase affecting mass uniformity. In addition to void fraction, percent difference in mass flow rate was also calculated and plotted in Figure 5 to identify mass uniformity at the distributor exits. It was noted that evaporation temperature of -8°C seems to provide most uniform mass flow rate distribution compared to -18°C and -25°C evaporation temperatures. However, percent difference in mass flow rate for three evaporation temperatures studied nearly stayed within 15% implying that evaporator distributor exits could supply acceptable mass uniformity although evaporation temperature changed from -8°C to -25°C.

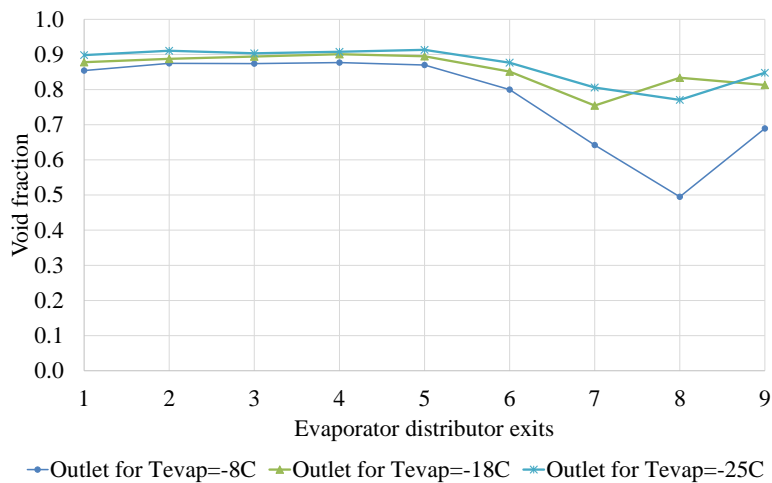


Figure 4. R404A outlet void fraction at evaporator distributor exits for evaporation temperatures of -8°C, -18°C and -25°C (nozzle position at 0.01mm).

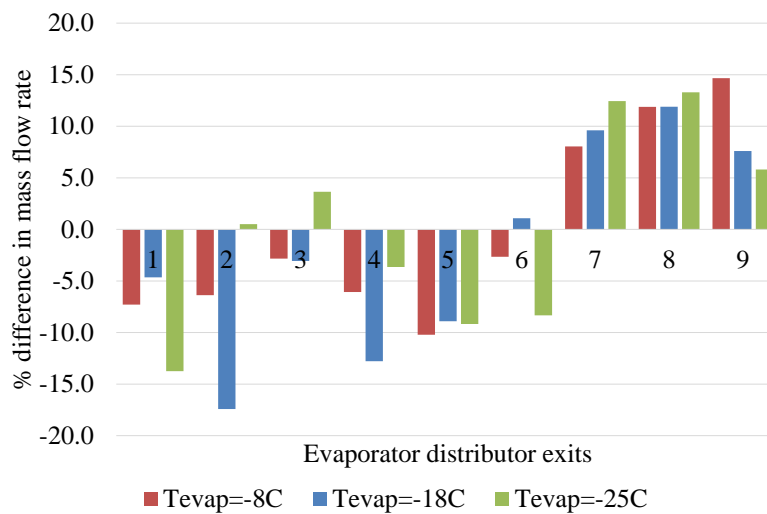


Figure 5. R404A % difference in mass flow rate at evaporator distributor exits for evaporation temperatures of -8°C, -18°C and -25°C (nozzle position at 0.01mm).

3.2. The effect of nozzle position on mass flow rate distribution for R404A

In this section of the study, distance between apex of distributor conical member and nozzle outlet was changed from 0.01 mm to 2.01 mm and 4.01 mm to understand the effect of distance on mass flow distribution at the evaporator distributor exits. Figure 6 and 7 show outlet void fraction and % difference in R404A mass flow rate values at evaporator distributor exits, respectively for nozzle positions of 0.01 mm, 2.01 mm and 4.01 mm. It was noted that void fraction values for exit numbers 7, 8 and 9 are significantly smaller than exit numbers of 1 thru 6. This implies that when void fraction decreases, vapor area in the mixture decreases as well and this yields increase in liquid area. Therefore, increase in % difference in mass flow rate for exit numbers of 7, 8 and 9 can be observed from Figure 7. Besides, it appears that 2.01 mm and 4.01 mm positions cause up to 40% difference in mass flow rate distribution. This may be due to fact that when distance between apex of distributor conical member and nozzle outlet is large, liquid and vapor mixture would separate from each other because of density differences and this would directly affect mass uniformity at the distributor exits.

Exit number 8 is at the bottom yielding highest deviation from averaged mass flow rate.

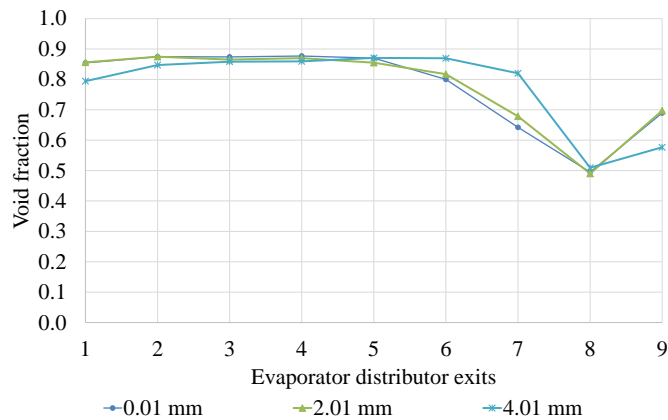


Figure 6. R404A outlet void fraction at evaporator distributor exits for nozzle positions of 0.01 mm, 2.01 mm and 4.01 mm (for evaporation at -8°C).

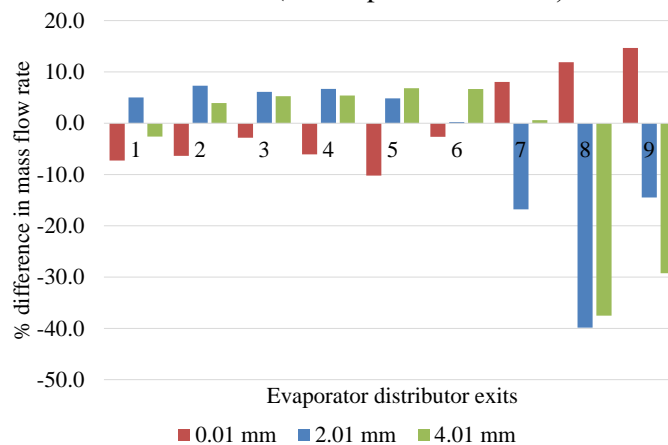


Figure 7. R404A % difference in mass flow rate at evaporator distributor exits for nozzle positions of 0.01 mm, 2.01 mm and 4.01 mm (for evaporation at -8°C).

3.3. The effect of evaporation temperature on mass flow rate distribution for CO_2

In addition to R404A, CO_2 was also studied in the present study to evaluate the use of a natural refrigerant on mass uniformity at the evaporator distributor. Figure 8 and 9 show outlet void fraction and % difference in CO_2 mass flow rate values at evaporator distributor exits, respectively for evaporation temperatures of -8°C , -18°C and -25°C . Outlet void fraction distribution of CO_2 was obtained quite different than that of R404A since outlet void fraction fluctuates between void fractions of 0.3 to 0.7 for these evaporation temperatures. Furthermore, these fluctuations in void fraction caused only 5% difference in mass flow rate at the exits except for exit number 9. This indicated that more uniform mass flow rate can be achieved when CO_2 is preferred to be used instead of R404A.

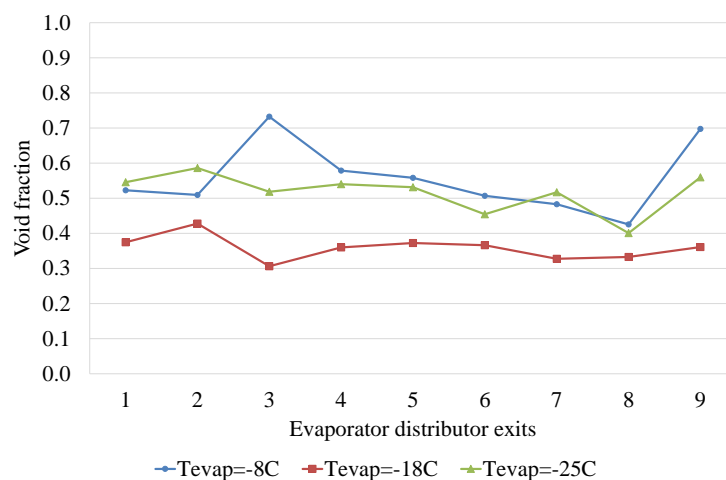


Figure 8. CO_2 outlet void fraction at evaporator distributor exits for evaporation temperatures of -8°C , -18°C and -25°C (nozzle position at 0.01mm).

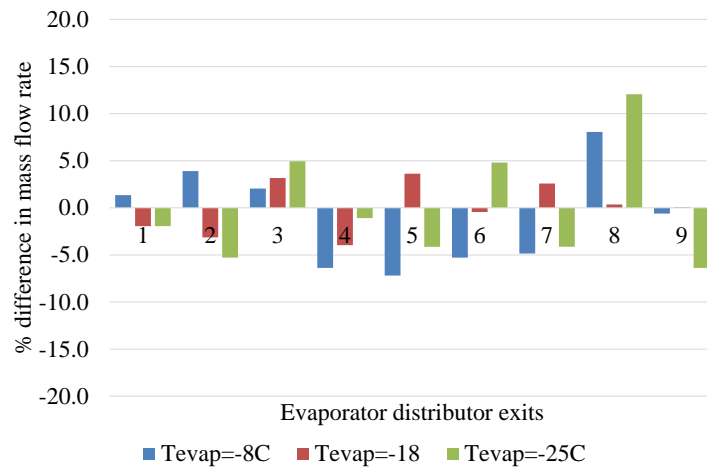


Figure 9. CO₂ % difference in mass flow rate at evaporator distributor exits for evaporation temperatures of -8°C, -18°C and -25°C (nozzle position at 0.01mm).

3.4. The effect of nozzle position on mass flow rate distribution for CO₂

The effect of nozzle placement in the evaporator distributor was also evaluated for CO₂. Figure 10 and 11 illustrate outlet void fraction and % difference in CO₂ mass flow rate values at evaporator distributor exits, respectively for nozzle positions of 0.01 mm, 2.01 mm and 4.01 mm. It was noted outlet void fraction stayed between 0.4 and 0.75 for all the nozzle positions. This variation in outlet void fraction resulted in nearly uniform mass flow rate at the evaporator distributor indicating that space variation of nozzle position had negligible influence on mass flow rate uniformity at the exits. Specifically, % difference in mass flow rate stayed less than 10% regardless of the nozzle positions.

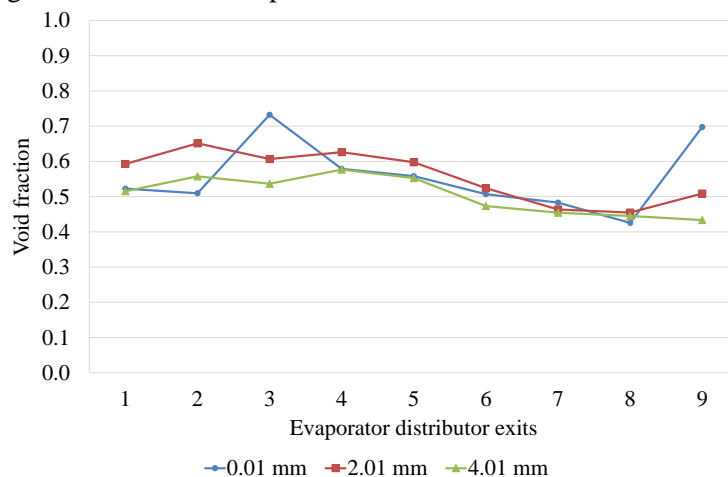


Figure 10. CO₂ outlet void fraction at evaporator distributor exits for nozzle positions of 0.01 mm, 2.01 mm and 4.01 mm (for evaporation at -8°C).

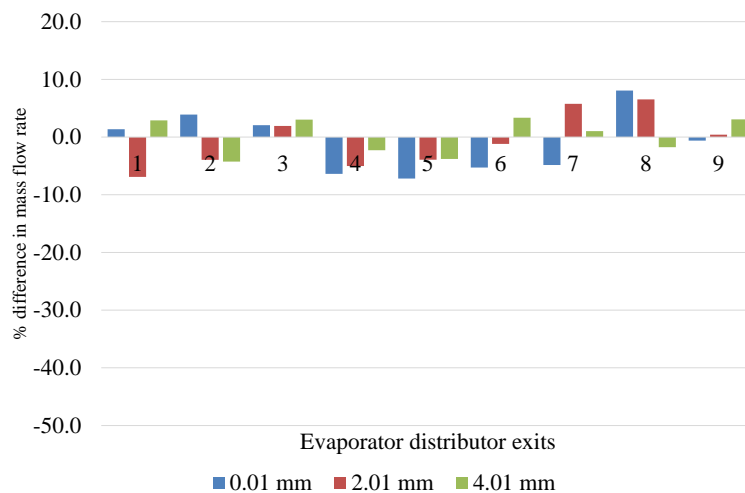


Figure 11. CO₂ % difference in mass flow rate at evaporator distributor exits for nozzle positions of 0.01 mm, 2.01 mm and 4.01 mm (for evaporation at -8°C).

4. CONCLUSION

In the present study, mass flow rate uniformity at an evaporator distributor exits was investigated at three different evaporation temperatures and nozzle placements. Two different refrigerants, R404A and R744 (CO₂) were used in generated three dimensional computational fluid dynamics models. Thermophysical characteristics of both refrigerants are determined based on the assumption that both coolers are performing the same cooling capacity. Effect of evaporation temperature was only significant for R404A study since -8°C evaporation temperature provided most uniform mass uniformity at the distributor exit. It was also realized that nozzle positions of 0.01, 2.01 and 4.01 mm were only significant for R404A fluid flow simulations since both 2.01 and 4.01 mm nozzle locations resulted in nearly 40% deviation in mass flow rate at distributor exits. Furthermore, % difference in mass flow rate results implied that use of nozzle position 1.01 mm could benefit better mass flow uniformity at the distributor exits compared to other studied nozzle positions. On the other hand, CO₂ simulations indicated nearly no significant differences in mass flow rate uniformity for different positions of nozzle.

REFERENCES

- Aziz, A., Miyara, A., & Sugino, F. (2012). Distribution of two-phase flow in a distributor. *Journal of Engineering Science and Technology*, 7(1), 41–55.
- Balasubramaniam, R., Ramé, E., Kizito, J., & Kassemi, M. (2006). Two Phase Flow Modeling: Summary of Flow Regimes and Pressure Drop Correlations in Reduced and Partial Gravity. *Nasa*, (January), 214085.
- Bowers, C. D., Wrocklage, D., Division, P. S., & Elbel, S. (2014). Improvements in Refrigerant Flow Distribution Using an Expansion Valve with Integrated Distributor.
- Equation, Z. T., & Models, T. (1993). Zonal Two Equation k- ϵ , Turbulence Models for Aerodynamic Flows . Florian R . Menter E lo ret I nst i t u t e , S u n n y v a l e . Mailing Address : 24th Fluid Dynamics Conference ZONAL TWO EQUATION k - ϵ TURBULENCE MODELS FOR AERODYNAMIC FLOWS.
- Fei, P., & Hrnjak, P. S. (2004). Adiabatic developing two-phase refrigerant flow in manifolds of heat exchangers, *61801*(217). Retrieved from <https://www.ideals.illinois.edu/handle/2142/12316>
- Kim, J. H., Braun, J. E., & Groll, E. A. (2009). Evaluation of a hybrid method for refrigerant flow balancing in multi-circuit evaporators. *International Journal of Refrigeration*, 32(6), 1283–1292. <https://doi.org/10.1016/j.ijrefrig.2009.01.016>
- Li, G., Braun, J. E., Groll, E. A., Frankel, S., & Wang, Z. (2002). Evaluating the performance of refrigerant flow distributors. *International Refrigeration and Air Conditioning Conference at Purdue*, R12-6.
- Li, G., Frankel, S. H., Braun, J. E., & Groll, E. A. (2002). Application of CFD models to two-phase flow in refrigerant distributors. *International Refrigeration and Air Conditioning Conference*, paper 592. <https://doi.org/10.1080/10789669.2005.10391125>
- Nakayama, M., Sumida, Y., Hirakuni, S., & Mochizuki, A. (2000). Development of a refrigerant two-phase flow distributor for a room air conditioner. *International Refrigeration and Air Conditioning Conference*.
- Poggi, F., Macchi-Tejeda, H., Maréchal, A., Leducq, D., & Bontemps, A. (2007). Experimental study of single and two-phase adiabatic flow distribution in compact heat exchangers. *18 Th France Congress of Mechanics Engineering*, 27–31. Retrieved from <http://documents.irevues.inist.fr/handle/2042/15987>
- Sökücü, M. H. (2016). *DİSTRİBÜTÖR GEOMETRİSİNİN EVAPORATÖR PERFORMANSINA ETKİSİNİN NUMERİK VE DENEYSEL İNCELENMESİ*. Yalova University.
- Tompkins, D., Yoo, T., Hrnjak, P., Newell, T., & Cho, K. (2002). Flow distribution and pressure drop in micro-channel manifolds. *International Refrigeration and Air Conditioning Conference, Paper 554*. Retrieved from <http://docs.lib.purdue.edu/cgi/viewcontent.cgi?article=1553&context=iracc>
- Wilcox, D. C. (1993). Turbulence Modelling for CFD: Index. *Turbulence Modeling for CFD*, 263–266.